



14th Deep Sea Offshore Wind R&D Conference, EERA DeepWind'2017, 18-20 January 2017, Trondheim, Norway

## Offshore Wind Turbine Wake characteristics using Scanning Doppler Lidar

R. Krishnamurthy<sup>a</sup>\*, J. Reuder<sup>b</sup>, B. Svoldal<sup>c</sup>, H. J. S. Fernando<sup>a</sup>, J. B. Jakobsen<sup>d</sup>

<sup>a</sup> University of Notre-Dame, Notre-Dame, Indiana, USA

<sup>b</sup> Geophysical Institute, University of Bergen, and Bjerknes Centre for Climate Research, Bergen, Norway

<sup>c</sup> Christian Michelson's Research Institute, Bergen, Norway

<sup>d</sup> University of Stavanger, Stavanger, Norway

---

### Abstract

Within an offshore wind park, wind flow characteristics are quite complex and govern both the energy production and the structural wind turbine response. An experimental study focussed on assessing the spatial variability of winds near the German offshore wind energy platform FINO1 was conducted using multiple remote sensing devices. This study focuses on measuring the wind turbine wake characteristics, such as velocity deficit, the extent (length and width) of the wake and wake meandering under various atmospheric conditions using the data collected from a single scanning Doppler Lidar for several months in 2016. A new algorithm based on using a Gaussian model to measure the downwind wake characteristics is developed. The wind turbine downwind wake deficits compared well to previous models at far-wake regions, while at near-wake regions the models deviated due to different instruments & methodologies used in measuring the wake characteristics. It was also observed that the length of the Alpha Ventus wind turbine wake varied from 3 to 15 times the Rotor Diameter (RD), and the maximum velocity deficit varied from 55% to 75% of the free-stream wind speed, depending on mean wind speed and atmospheric stability. Detailed analysis of the Alpha Ventus wind turbine wake characteristics is presented.

© 2017 The Authors. Published by Elsevier Ltd.  
Peer-review under responsibility of SINTEF Energi AS.

*Keywords:* Wakes; scanning Lidar; Offshore; FINO1 Platform

---

---

\* Corresponding author. Tel.: +1 574 631 3467; fax: +1 574 631 9236.  
E-mail address: [rkrishn1@nd.edu](mailto:rkrishn1@nd.edu)

## 1. Introduction

The effect of offshore wakes on wind turbines is a topic of increasing interest for several wind energy developers. Wind turbine spacing is majorly constrained by the effect of wind turbine wakes on downwind turbines. The improved quantification of the role of wind turbine spacing on power losses due to wind turbine wakes is a major focus of several companies. If the effect of turbine spacing on power losses and fatigue load due to wakes can be quantified, then this can be used to optimize wind farm layouts and thereby reduce the overall cost of a wind farm. Quantifying various characteristics of wake behavior, such as length, width, velocity deficit and wake meandering, is important for designing future wind parks as well as estimating its Annual Energy Production (AEP).

Measurements of the wind turbine wakes has been recently improved due to the use of remote sensing devices. These devices provide the ability to measure the complex flow of wind turbine wake interactions during various atmospheric conditions. Several studies have been conducted to measure the wake of a wind turbine using vertical remote sensing profilers (such as Lidars or Sodars) to estimate wake parameters at selected downwind distances from a wind turbine [1-3]. Commercial short-range vertical profilers provide accurate measurements of 10-minute averaged horizontal wind speed and wind direction given the atmosphere is spatially homogeneous. During inhomogeneous or complex flow conditions vertical profilers, which use Doppler Beam Swinging (DBS) techniques, provide less accurate measurements compared to standard *in-situ* measurements [4,5]. Although such profilers cover the entire rotor swept area at a given location, they do not have the capabilities to measure the entire 3-Dimensional (3D) wind turbine wake. Nacelle-mounted Lidars have proven to provide accurate mean wind ahead of the wind turbine [6,7], but have the same limitation as vertical profilers while measuring complex flows (assumes homogeneity of winds within a given range sector). Scanning Doppler Lidars can characterize wind flow over a large domain, ranging from several tens of kilometers [8-11] to 3-4 kilometers by recent fiber based coherent Doppler Lidars [12-15]. Scanning Doppler Lidars have proven the ability to estimate the length, width and deficit of wakes in a variety of atmospheric conditions [16-19].

To measure the wind turbine wake characteristics, a scanning Lidar can be placed on the nacelle of a wind turbine [18] or on a platform/ground a few hundred meters away from the wind turbine [17, 20], both these methods have their own advantages and disadvantages. The scanning Lidar measurements from a wind turbine nacelle provide hub-height view several kilometers downwind of the wind turbine but could be affected by the dynamic vibrations of the wind turbines thus resulting in large fluctuations in measurement height at longer distances. For example, a vibrational effect causing a  $\pm 0.2$ -degree deviation in the elevation angle will result in the Lidar measuring  $\pm 13.96$  m above or below the intended measurement height at 4 kilometers. Therefore, either appropriate motion stabilization platforms need to be designed for dynamically compensating the vibration from the wind turbines or appropriate algorithms should be developed to account for the dynamic change in elevation height between successive beams. Most modern fiber-optic based scanning Lidars cannot withstand the vibrational effects and could cause serious damage to the hardware unless appropriate measures are taken to secure the device to the wind turbine. Ground-based scanning Lidars do not provide constant hub-height measurements at all the downwind distances, due to higher elevation angles needed for measuring the hub-height, but provide more stable and reliable measurements over the duration of the campaign. For offshore conditions, the scanning Lidars can be placed on top of an existing platform which provides a reasonable height to scan the hub-height of modern wind turbines at low elevation angles. This would reduce the cost of deployment, provide measurements which are not affected by the vibrations of a wind turbine, and provide easy access to the instrument during installation/de-installation and troubleshooting, if required.

In this paper, results from an intensive offshore measurement campaign conducted from an offshore research platform will be presented. In particular, wind turbine wake measurements by a Windcube 100S scanning Doppler Lidar will be discussed. The Windcube 100S Lidar had the ability of measuring up to a distance of 3 kilometers, covering several wind turbines in its field of view. A new algorithm is developed to quantify several wake attributes such as the wind velocity deficit several hundred meters downwind of the wind turbine, length of the wind turbine wake and deviation of the wake centerline from scanning Lidar measurements. The details of the measurement

campaign setup and methodology are presented in Section 2 & 3, while the results and summary are presented in Section 4 & 5, respectively.

### Nomenclature

|       |   |
|-------|---|
| VD    | Velocity Deficit  |
| U     | Velocity inside the wake of the wind turbine                    |
| $U_A$ | Free-stream velocity outside the wake of the wind turbine       |
| $W_L$ | Length of the wind turbine wake                                 |
| $W_C$ | Wake centreline   |
| x     | Lateral distance perpendicular to the wind turbine              |
| $V_r$ | Doppler Lidar radial velocity                                   |
| u     | Zonal velocity  |
| v     | Meridional velocity   |
| w     | Vertical velocity   |
| RD    | Rotor Diameters   |
| D     | Downwind distance by rotor diameter [Non-dimensional parameter] |
| PPI   | Planned Position Indicator [constant elevation scans]           |
| RHI   | Range Height Indicator [constant azimuth scans]                 |
| MSL   | Mean Sea Level  |

## 2. Experiment Site & Setup

The OBLEX-F1 (Offshore Boundary-Layer Experiment at FINO1) campaign was performed at the German wind energy research platform FINO1, which is located approximately 45 kilometers off the German island Borkum in the North Sea (NORCOWE web page: <http://norcowe.no/>). The key purpose of the campaign was to gain improved knowledge of the marine atmospheric boundary-layer (MABL) affecting the performance and the production of the near-by wind farms. In order to provide a unique data set for boundary-layer stability in offshore conditions, simultaneous measurements of wind, temperature and humidity profiles in the MABL were performed. The collected observational data will be used to validate and improve numerical models and tools e.g. weather forecasting, marine operations and wind farm layout optimizations (NORCOWE web page: <http://norcowe.no/>).

As part of a measurement campaign performed by the Norwegian Centre for Offshore Wind Energy (NORCOWE), two Windcube 100S, amongst others, were installed on the south-east side of the FINO1 platform in May 2015 (shown in Figure 1 & Table 1). In August 2016, exploratory tests were dedicated to wind turbine wakes by using a sequence of Planned Position Indicator (PPI) and Range Height Indicator (RHI) scans. Details on the specific scan patterns used for the analysis in this paper are shown in Section 2.2.

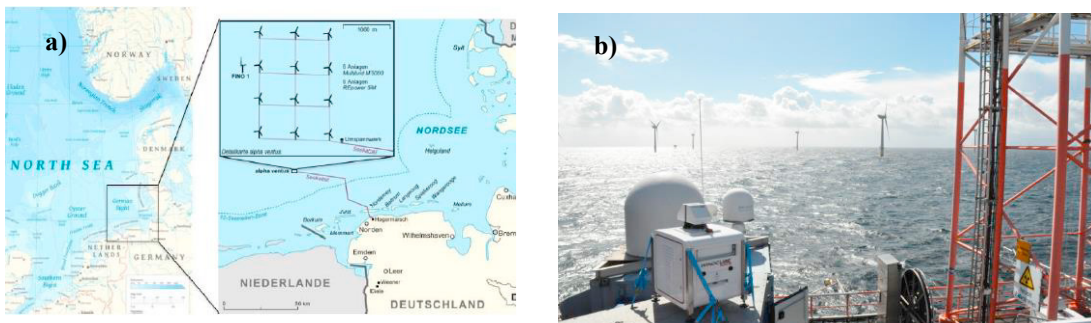


Fig. 1. (a) Alpha Ventus wind farm and the offshore wind farm orientation in North Sea near FINO1 platform (Wikipedia); (b) deployment of the scanning Doppler Lidar on the FINO1 platform overlooking the offshore wind farm (NORCOWE web page: <http://norcowe.no/>).

In this paper, measurements only from a single scanning Doppler Lidar are studied and the Lidar specifications are provided in Table 2. Future work would entail combining the measurements from several of the above mentioned measurements.

Table 1. Location of the Lidar and wind turbines

| Lidar/Wind Turbine      | UTM Easting (m) | UTM Northing (m) | Height (m) |
|-------------------------|-----------------|------------------|------------|
| Scanning Doppler Lidar  | 341942.58       | 5987859.17       | 23.5       |
| Turbine Hub Height AV4  | 342346.00       | 5987796.81       | 90         |
| Turbine Hub Height AV7  | 342341.25       | 5987036.05       | 90         |
| Turbine Hub Height AV10 | 342336.11       | 5986238.12       | 90         |

2.1. Meteorological Conditions

The FINO1 platform mast is instrumented to measure the horizontal wind speed, direction and temperature at several heights (33, 40, 50, 60, 70, 80 and 90 m above mean sea level (MSL)). During the months August to September 2016 (study period), the wind directions were predominantly from south – south west, as shown in Fig 2. The FINO1 met-mast is approximately 405 m away from the closest wind turbine at the Alpha Ventus wind farm. Due to the limitations in the proposed algorithm in Section 3 and location of the scanning Lidar relative to the wind turbines, measurements only from north – north westerly direction were used for the below analysis.

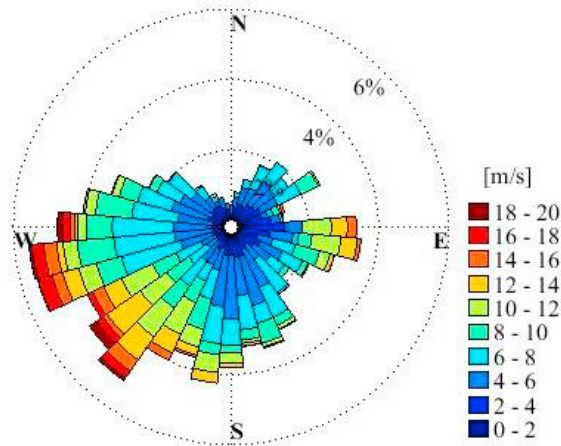


Fig 2. Wind rose of the FINO1 site for the months of August & September, 2016 at 90 m above MSL.

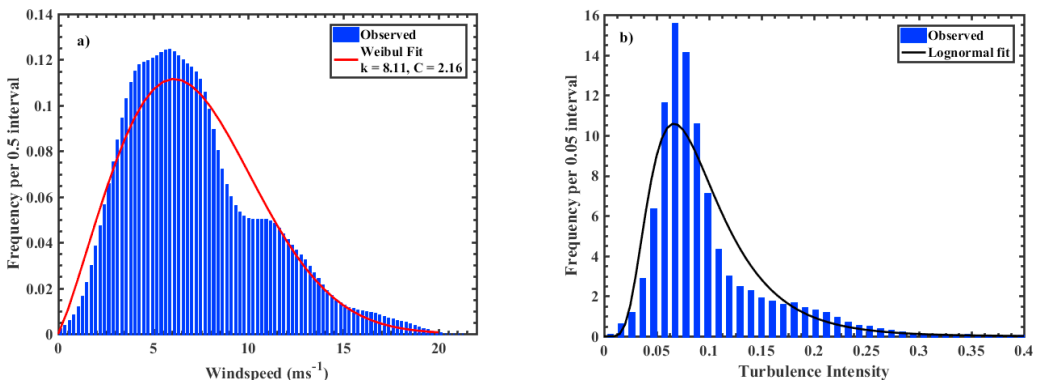


Fig 3. a) Horizontal wind speed probability distribution function at 90 m above MSL, showing a bi-modal distribution, and the Weibull fit shown in red for the months of August & September, 2016, b) Turbulence Intensity at 90 m for the same time period with a Log-normal fit.

The wind speed distribution, in Fig 3a, shows a mean wind speed of approximately 7.5 m/s for the months of August & September, 2016. A bi-modal distribution is observed in the data, with a Weibull shape parameter ( $k$ ) of 8.11 and scale parameter ( $C$ ) of 2.16. The wind industry standard Weibull fit does not provide an accurate fit to the data observed at FINO1. Low turbulence intensity, mostly less than 0.1, was also observed (shown in Fig. 3b).

## 2.2. Scanning Strategy

The scanning Lidar were placed on the FINO1 platform, which was 21 m above mean sea level. The hub-height of the Alpha Ventus AV7 to AV12 wind turbines is 90 m, with a rotor diameter of 116 m. The scanning Lidar performed repeated PPI scans at hub-height in the direction of AV7 Wind turbine (Fig 4). A 48-degree sector PPI scan was performed at an elevation angle of 4.62 degree with a scan rate of 1 degree per second (resulting in an azimuthal resolution of 15 m at wind turbine AV7), as shown in Table 3. This resulted in approximately 12 scan repetitions every 10 minutes. The range-gate size or radial resolution of the Lidar is 25 m, for dense measurements surrounding the wind turbine. Fig. 4 shows the scan coverage and the respective distances between the Lidar and Alpha Ventus wind turbines.

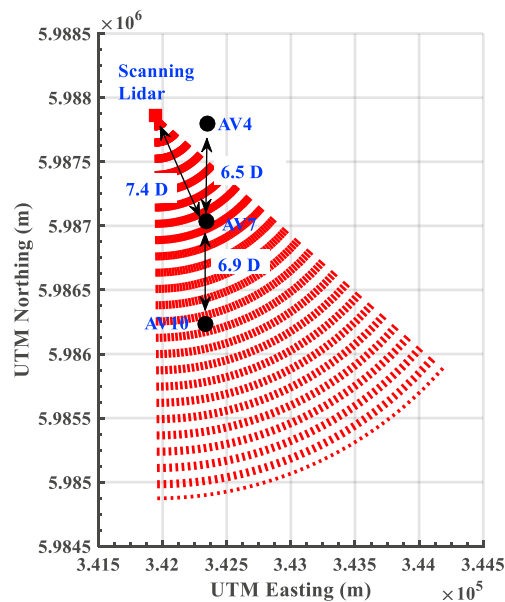


Fig. 4. Location of the wind turbines under investigation with respect to the scanning Doppler Lidar. The scan pattern used for the analysis is also displayed (dashed red lines).

Table 2. Windcube scanning Doppler Lidar Specifications

| Lidar Specifications                      | Value    |
|---|----------|
| Eye Safety                                | Class 1M |
| Wavelength ( $\mu\text{m}$ )              | 1.54     |
| Pulse Energy ( $\mu\text{J}$ )            | 100      |
| PRF (Hz)                                  | 10000    |
| Pulse Averaged                            | 10000    |
| Pulse Duration (ns)                       | 150      |
| Range-gate interval (m)                   | 25       |
| Velocity Precision ( $\text{cm s}^{-1}$ ) | < 20     |
| Minimum Range (m)                         | 50       |
| Maximum Range (m)                         | 3000     |

Table 3. Scan pattern for the data analyzed

| Scan Pattern                     | Azimuth<br>(deg) | Elevation<br>(deg) | Scan rate<br>(deg/sec) | Averaging<br>(secs) |
|----------------------------------|------------------|--------------------|------------------------|---------------------|
| Planned Position Indicator (PPI) | 131.5 – 179.5    | 4.62               | 1                      | 1                   |

### 2.3 Data Filtering

The scanning Lidar data was filtered based on the Carrier to Noise Ratio (CNR) of the instrument, as recommended by the manufacturer. A threshold of -24 dB was applied to further filter the data out, which removed significant amount of bad data. Due to the presence of wind turbines, the radial velocity surrounding the wind turbine also gets affected, also known as range-gate bleeding. When a part of the Lidar pulse, approximately 28 m for the Windcube 100S, hits a hard-target it creates a spike in the measurements. Therefore, the surrounding measurements along the radial and azimuthal direction are impacted by the range-gate bleeding. This results in spurious estimates of the radial velocity surrounding a hard-target and should be filtered. A gradient filter based on CNR jumps between successive beams and range-gates is used to remove the remainder of spurious data. In the analysis below the filtering methodology proposed in [21] is also used to filter out spurious radial velocity data.

### 3. Estimation of wind turbine wake parameters

The scanning Lidar provides a projection of the wind in the direction of the Lidar beam, which can be used to visualize and estimate various wake characteristics. The radial velocity measured by the Doppler Lidar is given by:

$$V_r = u \sin \phi \cos \theta + v \cos \phi \cos \theta + w \sin \theta \quad (1)$$

where,  $V_r$  is the radial velocity;  $[u, v, w]$  are the three components of wind speed,  $\phi$  is the azimuth angle and  $\theta$  is the elevation angle of the scanning Doppler Lidar. Therefore, if the wind direction is along the line of sight of the Lidar measurements the radial velocity is equal to the horizontal wind speed.

The wind turbines were located between 500 to 900 m away from the scanning Lidar which has a maximum acquisition range of 3000 m, and the true range depends on atmospheric conditions and aerosol loading at a given site. The methodologies implemented in [17] & [18] were partially used to estimate the wind turbine characteristics, such as the wind velocity deficit (VD), wake centerline ( $W_c$ ) and wake length ( $W_L$ ). The radial velocity measurements were averaged over 5 minutes for the results shown in this paper. Ideal conditions for this algorithm to work are:

1. The wind direction should be nearly aligned with the Lidar-turbine azimuth direction, since winds perpendicular to the Lidar-turbine axis would have radial velocities almost equal to zero. Therefore, only wind directions  $330 \pm 30$  degrees has been used in the analysis below.
2. The Lidar elevation angle should be focused close to hub-height of the wind turbine and lower elevation angles are preferred
3. The azimuth extent of the scan should be sufficiently large to cover the length of the wake (in this study a 48-degree sector width was used)

The velocity deficit (VD) of a wind turbine is defined as

$$VD(R, x) = \left(1 - \frac{U(R, x)}{U_A(R, x')}\right) \times 100\% \quad (2)$$

where  $U_A$  is the mean ambient wind speed outside of the wake,  $U$  is the mean wind speed within the wake downstream of the wind turbine,  $R$  is the downwind distance from the wind turbine,  $x$  is the lateral distance perpendicular to the wind turbine axis, and  $x'$  is the free-stream distance away from the wind turbine (1.6 D).

The various steps in the algorithm are detailed below:

1. The horizontal wind direction is calculated ahead of the wind turbine using the methodology described in [21]. The algorithm performs a single value decomposition of a sector of data ahead of the wind turbine. The output is averaged  $U$  &  $V$  components of the wind speed over the entire sector chosen (48 degrees for this setup), which is then used to estimate the horizontal wind direction. Fig. 5 shows the measurements from scanning Lidar, 100 m ahead of the wind turbine, and FINO1 met-mast, 7.4 Rotor Diameters (RD) ahead of the wind turbine at the same height (90 m above MSL).

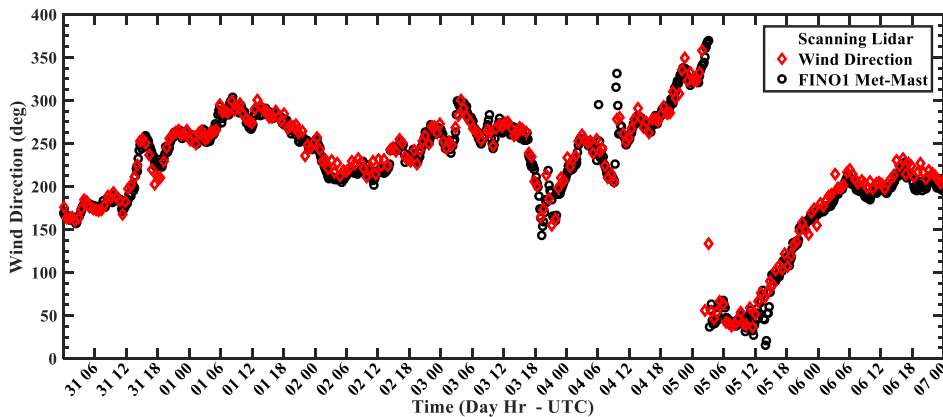


Fig.5. Horizontal wind direction measured ahead of the wind turbine by the scanning Lidar and FINO1 Met-mast at 90 m from August 31<sup>st</sup> to September 7<sup>th</sup>, 2016.

2. If the wind direction ( $\theta_v$ ) was measured to be within  $330^\circ \pm 30$  degrees ahead of the wind turbine, then
  - a. The downwind locations, as shown in Fig. 6, along the center-axis of the wind turbine wake ( $R$ ) is identified based on the wind direction ahead of the wind turbine [17].
  - b. The location of the free-stream wind speed ( $U_A$ ) is identified as 1.6 RD away from the turbine's wake center-axis in the predominant wind direction, i.e.,  $U_A(R) = U(R', 1.6 \text{ RD})$ .
  - c. To estimate the center of the wind turbine wake, measurements from a perpendicular axis ( $x'$ ) spanning 250 m from the wind turbine center-axis ( $R$ ) is collected.

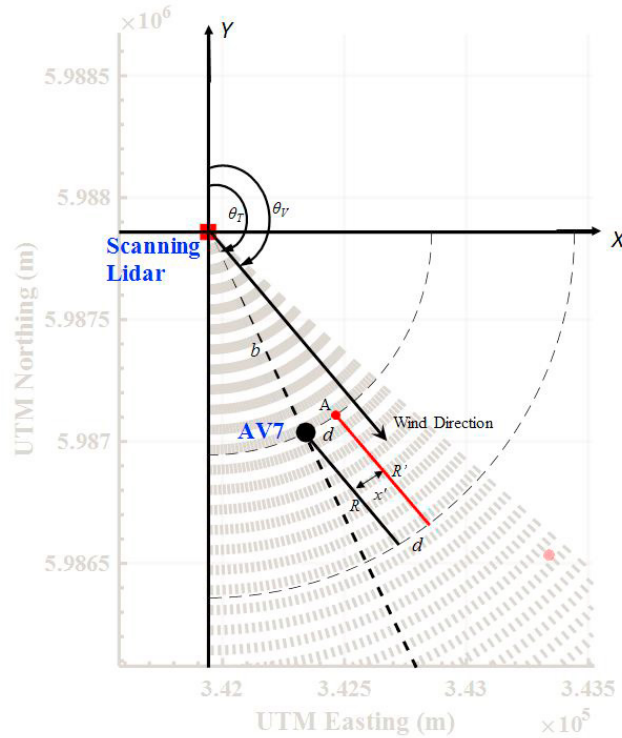


Fig 6. Illustration of the Doppler Lidar scan to determine the AV7 wind turbine’s wake locations downwind of the wind turbine. The wind direction  $\theta_v$  is calculated from lidar data ahead of the wind turbine and the direction between the Lidar and turbine is given as  $\theta_T$  with distance  $b$ . The free-stream wind speeds are measured parallel to the wake direction, from point A, separated by distance  $x'$ .

- d. A Gaussian fit is applied to the measurements along the perpendicular axis, to estimate the velocity deficit. The velocity deficit is defined as

$$VD_{fit}(R, x) = K e^{-\left[\frac{x-B}{c}\right]^2} \tag{3}$$

where  $K$ ,  $B$  &  $C$  are coefficients of the fit. The location of the maximum velocity deficit was used to estimate the center of the wake ( $W_c$ ) at all downwind distances. The Gaussian fit to the velocity deficit estimated at multiple downwind distances from the wind turbine is shown in Fig. 7. The wake centerline ( $W_c$ ) is then defined as

$$W_c(R) = \max[VD_{fit}(R, x)] \tag{4}$$

- e. The wind turbine wake length ( $W_L$ ) is defined as the distance when the velocity deficit reaches less than 5% of the free-stream wind velocity. Fig. 8c shows velocity deficit as a function of rotor diameters downwind of the wind turbine.

$$W_L = VD_{fit}(R, x) \leq 5\% \tag{5}$$



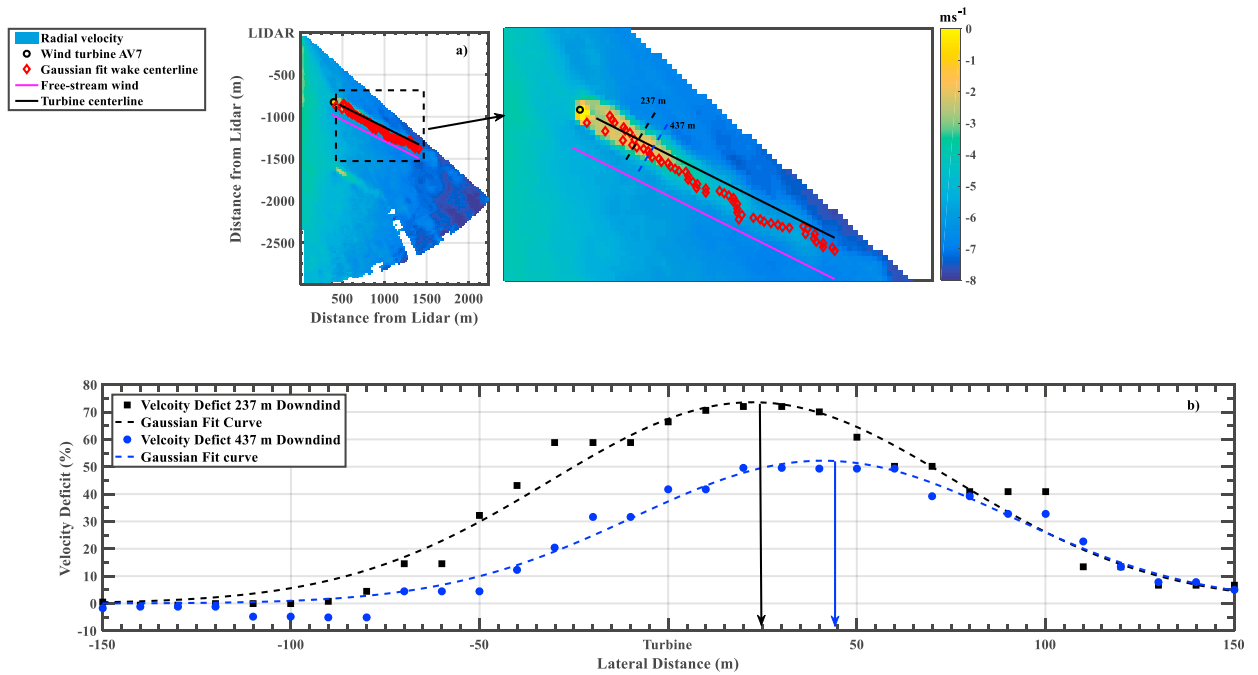


Fig. 7. a) Scanning Lidar radial velocity plot on September 8<sup>th</sup>, 2016 at 2200 UTC with a zoomed in view of the wind turbine wake, wake centerline as estimated by the Gaussian fit (open red diamond), free-stream wind speed location (magenta line), wind turbine centerline (black line) [In this plot: negative radial velocity is winds going away from the Lidar and positive radial velocity is winds coming towards the Lidar]. The lateral cross-sections at 237 m and 437 m downwind of the turbine is also shown. b) the Gaussian fit (Equation 3) on the velocity deficit estimated as shown in Equation 2 at 237 & 437 m downwind of the wind turbine. The lateral location at the maximum velocity deficit is estimated as the wake centerline.

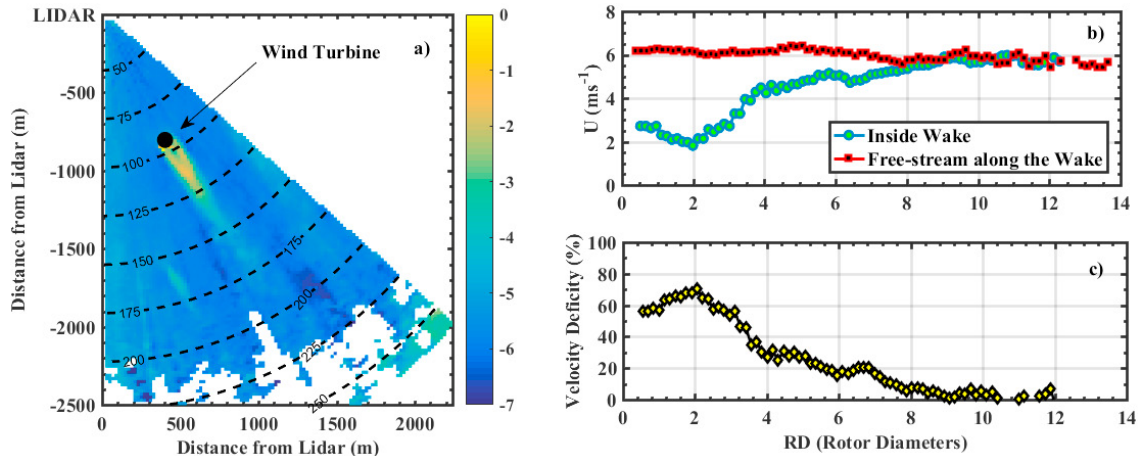


Fig. 8. a) Scanning Lidar measurements of wind turbine wake at FINO1 on September 9<sup>th</sup>, 2016 at 0900 UTC. The colors depict the filtered radial velocity obtained from scanning Lidar measurements and the dotted lines show the height above mean sea level [In this plot: negative radial velocity is winds going away from the Lidar and positive radial velocity is winds coming towards the Lidar], b) velocity observed inside and outside the wake of the wind turbine and c) calculated velocity deficit at several downwind distances.

Our wake “geometry” observed is at an increasing height at an increasing distance from the wind turbine (contours in Fig 8a). If we assume that the wake has an idealized axisymmetric /conical shape, we could in future attempt a correction for a variable height, by increasing the observed wake width by a factor accounting for the difference between a (vertical

circle parallel to the rotor) diameter and a circle secant line. In this formulation, since the SCADA data was unavailable, the yaw error is assumed to be 0 i.e., the rotor plane is always assumed to be perpendicular to the flow.

#### 4. Results

Offshore wind turbine wakes generally decay more slowly unlike onshore wind turbine wakes due to lower turbulence levels, requiring the offshore wind turbines to have larger separation distances when compared to the onshore wind turbines. This has major financial consequences due to the additional costs for underwater cabling, operational & maintenance (O&M) costs etc. Therefore, it is of interest for wind farm developers to evaluate the decay of wake with downwind distance from the wind turbine. Several studies have been performed in evaluating the decay of wake from single and multiple wind turbines [1, 17-20]. Aitken et al., 2013 summarized wake data from a number of onshore and offshore sites. The relative velocity deficit (VD) against downwind distance was given as:

$$\frac{\Delta U}{U_A} = 56D^{-0.57} \quad (6)$$

where  $\Delta U$  is the velocity difference between the mean stream wind speed ( $U_A$ ) and velocity at the wake of the wind turbine,  $D$  is the normalized downwind distance (i.e., the downwind distance from turbine by the rotor diameter).

The resolution of the Lidar data is 25 m in the radial direction and 15 m in the azimuthal direction (at the location of the turbine). This high resolution data revealed two trends in the velocity deficit, i) an increase of velocity deficit in the “near wake” region of the wind turbine up to 2 RD and ii) an exponential decay of velocity deficit till it reaches free-stream velocity. Fig. 9 shows the average velocity deficit over the period of study as a function of downwind distance. The magnitude of velocity deficit depends on the mean incoming wind speed, coefficient of Thrust ( $C_t$ ) of the wind turbine, atmospheric stability of the surrounding region and interaction of the wake with the neighbouring wind turbines. Therefore, Fig. 9 shows the average trends, over 252 samples, observed during summer time periods (August – September, 2016) at the FINO1 platform. Approximately 40% of the overall data was determined invalid, since the turbine was turned off. This was determined by removing data which have less than 20% velocity deficit within 2 rotor diameters downwind of the wind turbine.

To compare the data obtained with other field experiments shown above, a regression fit to the data was performed. The fit to the near-wake data ( $< 2$  RD) is shown in Equation 7 below

$$\frac{\Delta U}{U_A} = 0.65D^{0.09} \quad (7)$$

and the far wake mode ( $> 2$  RD) is shown in Equation 8 below

$$\frac{\Delta U}{U_A} = 1.50D^{-1.12} \quad (8)$$

The Coefficient of Correlation ( $R^2$ ) between the model and far & near wake data are 94.5% and 87.45%, respectively. Fig. 9 also overlays the observed fit to the data and other field experiments. Previous models were based on measuring wind speed deficits at select downwind distances using vertical profilers or tall met-masts. Further, fewer samples were available to develop statistically significant models. As shown in [4], the DBS approach that has been used to characterize wind turbine wakes using Sodars or vertical Lidar profilers can result in higher uncertainties of wind speed measurements due to the inhomogeneous flow inside the turbine wake region. An error of  $1 \text{ ms}^{-1}$  in wind speed estimation can result in approximately 10% difference in velocity deficit. Therefore, the uncertainty of the previous field experiments without a scanning Doppler Lidar could underestimate the overall velocity deficit of the wind turbine wake. The results shown in Fig. 8 are closer to visual trends observed from [17, 18], where

measurements from a scanning Doppler Lidar was used to estimate the velocity deficit, but no models were established in [17,18], hence they cannot be compared.

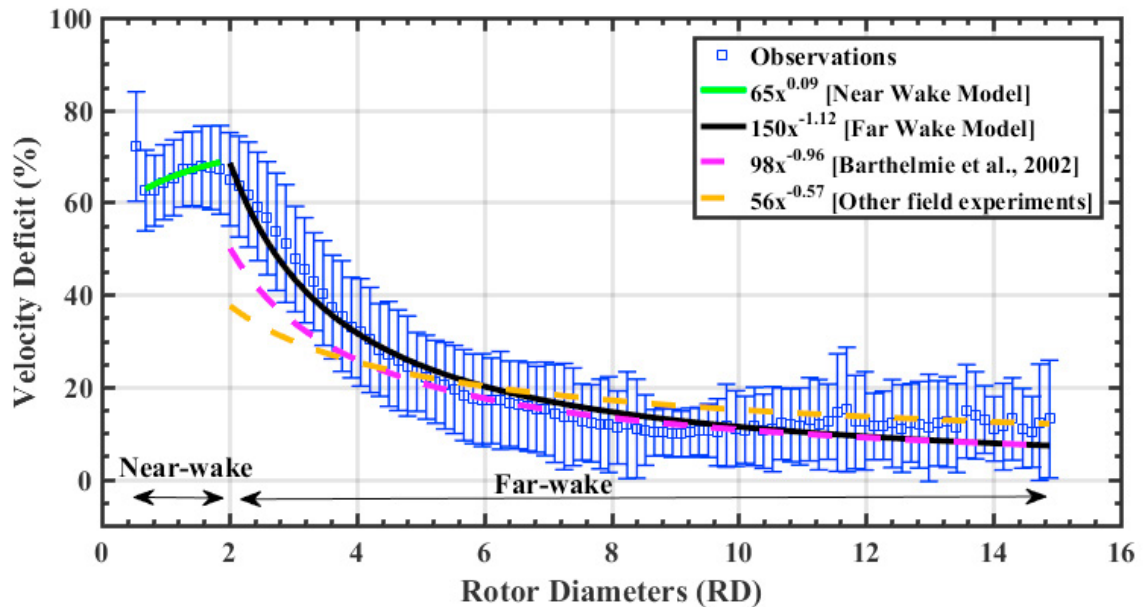


Fig. 9. Average wind turbine wake velocity deficit, 252 samples, as a function of normalized downwind distance (in Rotor Diameter [RD]) from the wind turbine. The error bars indicate one standard deviation of all the samples. Various other proposed models from existing literature are shown as reference.

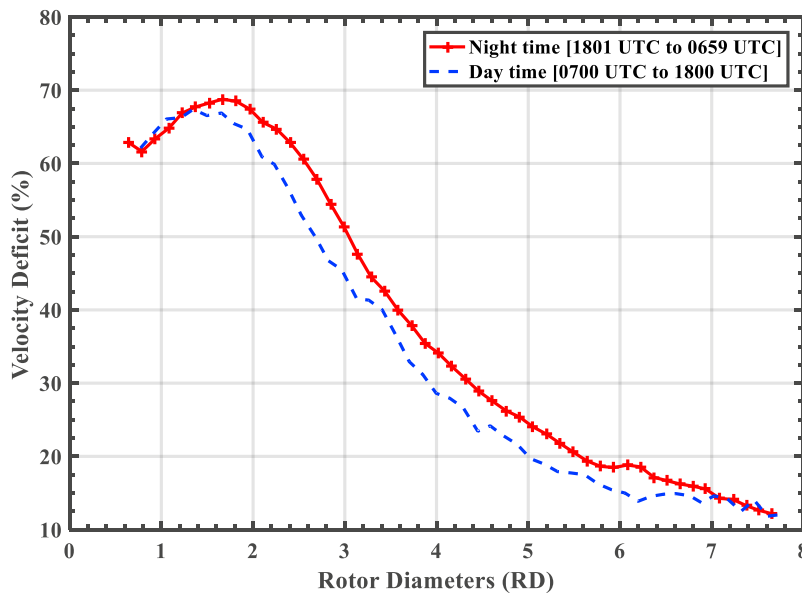


Fig. 10. Observed velocity deficit during day (0700 UTC to 1800 UTC, 154 samples) and night time (1801 UTC to 0659 UTC, 98 samples). Scanning Lidar retrieved velocity deficits from August to September, 2016.

Fig. 10 shows the velocity deficit observed during daytime and night time. The velocity deficit during night time is approximately 4-11% greater than velocity deficit observed during day time for the AV7 wind turbine at FINO1

platform. The maximum velocity deficit during daytime conditions is observed to reach at around 1.3 RD (176.8 m) downwind while at night time it is observed at 1.7 RD (231.2 m) downwind of the turbine. In offshore conditions, the Sea Surface Temperature (SST) during summer months does not vary much when compared to land surface temperatures. Therefore, the effect of daytime and night time variability could be different for both cases, but generally depends on the geographic location and other atmospheric conditions. Fig. 11 shows wind turbine wakes observed during two instances, shorter wake during daytime and longer wake during night time. The velocity deficit persists over a longer distance during night time, sometimes greater than 15 RD (Fig. 12). During daytime conditions the wake length is observed to vary between 3RD to 7RD (as shown in Fig. 11 & 12). Wake length of a single wind turbine is generally a function of 1) Incoming wind speed and thrust coefficient ( $C_t$ ) and 2) atmospheric stability parameters. For offshore conditions, the thermal stratification is low, due to lesser temperature gradient between the air and ocean, while the effect of wind shear is high. The high wind shear could result in larger wake lengths in offshore conditions. Therefore, the variability of wake lengths observed during day and night time can be attributed to increased shear conditions observed in FINO1. This will need to be investigated further and is currently beyond the scope of this study.

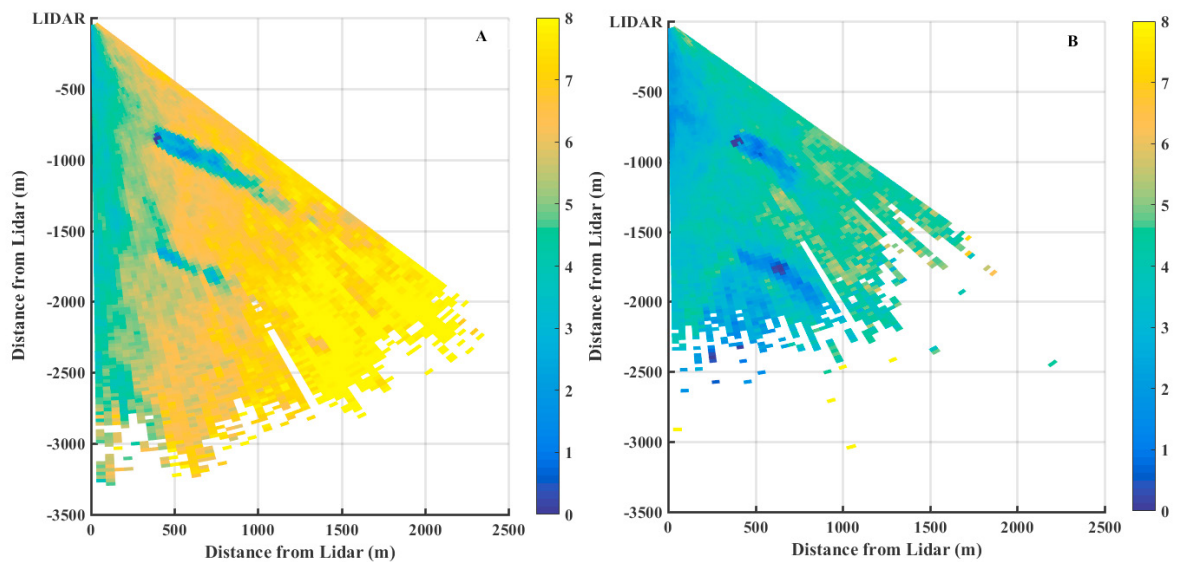


Fig. 11. A) Scanning Lidar measurements during night time on 8<sup>th</sup> September 2016 at 2200 UTC, B) Scanning Lidar measurements during daytime on 11<sup>th</sup> September 2016 at 0900 UTC. The radial velocity convention used in this plot is: positive radial velocity measurements are winds going away from the Lidar and negative measurements are winds going towards the Lidar.

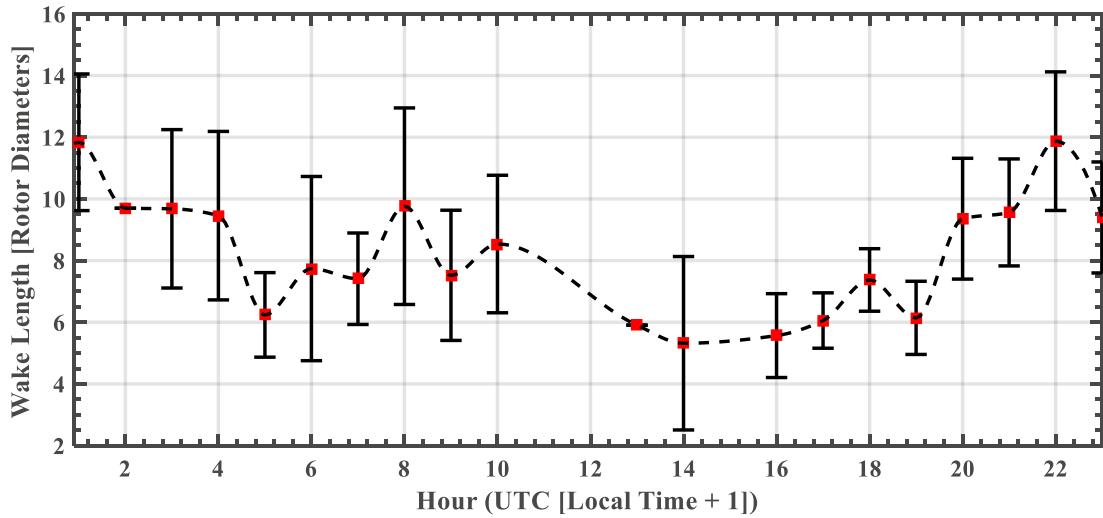


Fig. 12. One-hour averaged wake lengths measured by scanning Doppler Lidar at various times of the day for the data from August to September, 2016. The standard deviation ( $\pm 1\sigma$ ) of the mean is shown by error bars.

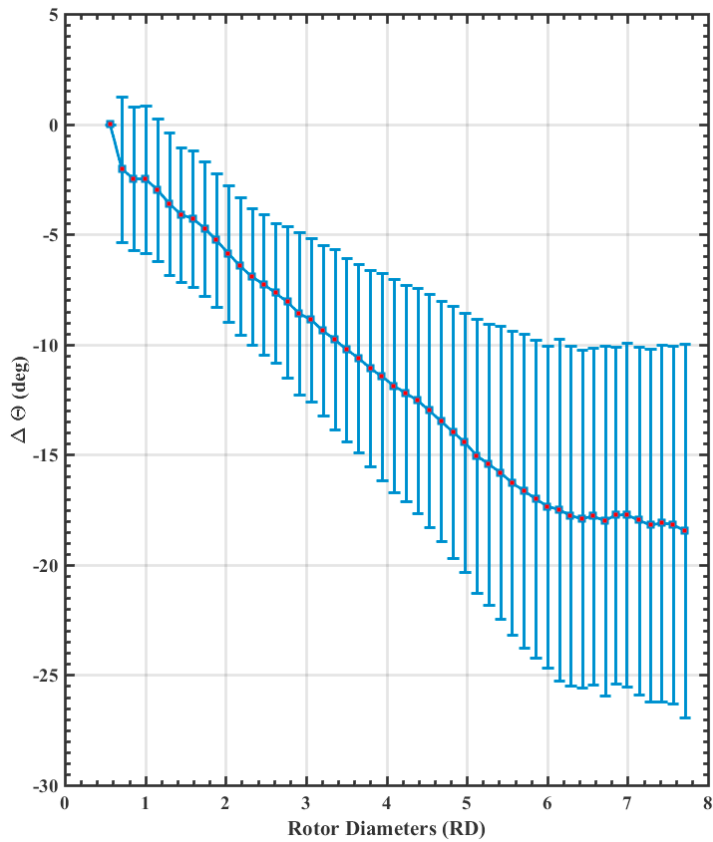


Fig. 13. Average deviation in degrees of the true wake center along the wind turbine wake centerline. The measurements are averaged for scanning Lidar measurements from August to September of 2016.

The wake centerline as estimated using the Gaussian fit, shows that the wake meandering was significant during the study period. Fig. 13 shows the deviation of the wind turbine wake centerline from the wind turbine axis. It was observed that a maximum deviation of approximately 20 deg from the wind turbine wake centerline was observed. This is significant and is a salient factor for future development of wind farm control techniques using wake re-direction [21-24] and designing future offshore wind farms.

## 5. Conclusions

The wind turbine wake characteristics observed at FINO1 showed interesting attributes of the behavior of offshore wakes. The wind turbine wake detection algorithm, which uses ground based Doppler Lidar for estimating the various characteristics of the wind turbine wakes, behaves well and provides deeper insights into the dynamic behavior of the wind turbine wakes. Unlike the nacelle mounted scanning Lidar, the ground based scanning Lidar provide steady measurements and are not affected by the vibrations from the wind turbines. Although the wake geometry of ground based Lidars increases with height, it provides undisturbed measurements which are needed for analyzing complex wake flows. Two empirically derived wind turbine wake models are proposed based on proximity to the wind turbine. These models are specific to the Alpha Ventus wind turbines and specific to the region. Previous wake models showed similar trends at far-wake regions, compared to near-wake regions. The effect of day and night time showed interesting trends for offshore conditions. The night time wake lengths were observed to be larger than the daytime wake lengths. This could be attributed to possible high shear and low thermal stratification conditions compared to onshore locations. Further investigation of the effect of offshore stratification and shear needs to be studied using modified Richardson number profiles within the wake of the wind turbine.

Instruments such as scanning coherent Doppler Lidars help bridge the gap between models and observations. The use of scanning Doppler Lidar for continuous monitoring of the wind farm is gaining interest, and integration of advanced algorithms to continuously track the dynamic wake characteristics would aide in improving wind farm performance.

## Acknowledgements

The OBLEX-F1 campaign was performed within the NORCOWE (Norwegian Centre for Offshore Wind Energy) project funded by the Research Council of Norway (RCN) under project number 193821. The wind lidars used for the analysis are part of the National Norwegian infrastructure project OBLO (Offshorer Boundary Layer Observatory) also funded by RCN under project number 277770. The authors would like to thank BMWi (Bundesministerium fuer Wirtschaft und Energie), Federal Ministry for Economic Affairs and Energy and the PTJ (Projektraeger Juelich, project executing organisation) for the FINO1 met-mast data. The authors would also like to thank Martin Flügge (CMR) for his assistance with data collection and correspondence.

## References

- [1] Barthelmie RJ, Larsen GC, Frandsen ST, Folkerts L, Rados K, Pryor SC, Lange B, Schepers G. Comparison of wake model simulations with offshore wind turbine wake profiles measured by sodar. *Journal of atmospheric and oceanic technology*. 2006 Jul;23(7):888-901.
- [2] Bingöl F, Mann J, Larsen GC. Light detection and ranging measurements of wake dynamics part I: one - dimensional scanning. *Wind energy*. 2010 Jan 1;13(1):51-61.
- [3] Trujillo JJ, Bingöl F, Larsen GC, Mann J, Kühn M. Light detection and ranging measurements of wake dynamics. Part II: two - dimensional scanning. *Wind Energy*. 2011 Jan 1;14(1):61-75.
- [4] Lundquist JK, Churchfield MJ, Lee S, Clifton A. Quantifying error of Lidar and sodar Doppler beam swinging measurements of wind turbine wakes using computational fluid dynamics. *Atmospheric Measurement Techniques*. 2015 Feb 23;8(2):907-20.
- [5] Newman JF, Bonin TA, Klein PM, Wharton S, Newsom RK. Testing and validation of multi - Lidar scanning strategies for wind energy applications. *Wind Energy*. 2016 Jan 1.
- [6] Kumar AA, Bossanyi EA, Scholbrock AK, Fleming P, Boquet M, Krishnamurthy R. Field Testing of LIDAR Assisted Feedforward Control Algorithms for Improved Speed Control and Fatigue Load Reduction on a 600kW Wind Turbine. *EWEA Annual Event, Paris, France*. 2015 Nov.
- [7] Schlipf D, Raach S, Haizmann F, Cheng PW, Fleming P, Scholbrock A, Krishnamurthy R, Boquet M. Adaptive Data Processing Technique for Lidar-Assisted Control to Bridge the Gap between Lidar Systems and Wind Turbines: Preprint. *NREL (National Renewable Energy Laboratory (NREL), Golden, CO (United States))*; 2015 Dec 14.

- [8] Krishnamurthy R, Calhoun R, Billings B, Doyle J. Wind turbulence estimates in a valley by coherent Doppler lidar. *Meteorological Applications*. 2011 Sep 1;18(3):361-71.
- [9] Krishnamurthy R, Choukulkar A, Calhoun R, Fine J, Oliver A, Barr KS. Coherent Doppler Lidar for wind farm characterization. *Wind Energy*. 2013 Mar 1;16(2):189-206.
- [10] Banakh V, Smalikho I. Coherent Doppler wind Lidars in a turbulent atmosphere. Artech House; 2013 Sep 1.
- [11] Banta RM, Pichugina YL, Brewer WA, Lundquist JK, Kelley ND, Sandberg SP, Alvarez II RJ, Hardesty RM, Weickmann AM. 3D volumetric analysis of wind turbine wake properties in the atmosphere using high-resolution Doppler Lidar. *Journal of Atmospheric and Oceanic Technology*. 2015 May;32(5):904-14.
- [12] Barthelmie RJ, Crippa P, Wang H, Smith CM, Krishnamurthy R, Choukulkar A, Calhoun R, Valyou D, Marzocca P, Matthiesen D, Brown G. 3D wind and turbulence characteristics of the atmospheric boundary layer. *Bulletin of the American Meteorological Society*. 2014 May;95(5):743-56.
- [13] Rhodes ME, Lundquist JK. The effect of wind-turbine wakes on summertime US Midwest atmospheric wind profiles as observed with ground-based doppler Lidar. *Boundary-Layer Meteorology*. 2013 Oct 1;149(1):85-103.
- [14] Krishnamurthy R, Boquet M, Osler E. Current Applications of Scanning Coherent Doppler Lidar in Wind Energy Industry. *INEPJ Web of Conferences 2016 (Vol. 119, p. 10003)*. EDP Sciences.
- [15] Vasiljević N, Lea G, Courtney M, Cariou JP, Mann J, Mikkelsen T. Long-range WindScanner system. *Remote Sensing*. 2016 Oct 29;8(11):896.
- [16] Käsler Y, Rahm S, Simmet R, Kühn M. Wake measurements of a multi-MW wind turbine with coherent long-range pulsed Doppler wind Lidar. *Journal of Atmospheric and Oceanic Technology*. 2010 Sep;27(9):1529-32.
- [17] Smalikho IN, Banakh VA, Pichugina YL, Brewer WA, Banta RM, Lundquist JK, Kelley ND. Lidar investigation of atmosphere effect on a wind turbine wake. *Journal of Atmospheric and Oceanic Technology*. 2013 Nov;30(11):2554-70.
- [18] Aitken ML, Banta RM, Pichugina YL, Lundquist JK. Quantifying wind turbine wake characteristics from scanning remote sensor data. *Journal of Atmospheric and Oceanic Technology*. 2014 Apr;31(4):765-87.
- [19] Ainslie, J. F.: Calculating the flow field in the wake of wind turbines. *J. Wind Eng. Ind. Aerodyn.*, 1988, 27, 213–224
- [20] Crespo A, Hernandez J, Frandsen S. Survey of modelling methods for wind turbine wakes and wind farms. *Wind energy*. 1999 Jan 1;2(1):1-24.
- [21] Kumer VM, Reuder J, Svardal B, Sætre C, Eecen P. Characterisation of single wind turbine wakes with static and scanning WINTWEX-W Lidar data. *Energy Procedia*. 2015 Dec 31; 80:245-54.
- [22] Krishnamurthy R. Wind farm characterization and control using coherent Doppler Lidar, 2013, 201 pp, PhD diss, Arizona State University. [https://repository.asu.edu/attachments/110579/content/Krishnamurthy\\_asu\\_0010E\\_12993.pdf](https://repository.asu.edu/attachments/110579/content/Krishnamurthy_asu_0010E_12993.pdf)
- [23] Barthelmie RJ, Hansen K, Frandsen ST, Rathmann O, Schepers JG, Schlez W, Phillips J, Rados K, Zervos A, Politis ES, Chaviaropoulos PK. Modelling and measuring flow and wind turbine wakes in large wind farms offshore. *Wind Energy*. 2009 Jul 1;12(5):431-44.
- [24] Fleming PA, Gebraad PM, Lee S, van Wingerden JW, Johnson K, Churchfield M, Michalakes J, Spalart P, Moriarty P. Evaluating techniques for redirecting turbine wakes using SOWFA. *Renewable Energy*. 2014 Oct 31; 70:211-8.